Robust Molecular Communications: DFE-SPRTs and Synchronisation

Tze-Yang Tung and Urbashi Mitra

Ming Hsieh Department of Electrical Engineering, University of Southern California, USA

Email: {tzeyangt,ubli}@usc.edu

Abstract-Precise synchronisation of transmitters and receivers is particularly challenging in diffusive molecular communication environments. To this end, a point-to-point molecular communication system is examined wherein the design of the transceiver offers resilience to synchronisation errors. In particular, the development of a sequential probability ratio test-based detector, which allows for additional observations in the presence of uncertainty due to mis-synchronisation at the receiver, and a modulation design which is optimised for this receiver strategy, is considered. The structure of the probability of molecules hitting a receiver within a particular time slot is exploited. An approximate maximum log-likelihood estimator for the synchronisation error is derived and the Cramér-Rao bound (CRB) computed, to show that the performance of the proposed estimator is close to the CRB at low transmission rates. The proposed receiver and modulation designs achieve strongly improved asynchronous detection performance for the same data rate as a decision feedback based receiver by a factor of 3 to 5 on average.

Index Terms—molecular communication, diffusion, sequential probability ratio test, sequence optimisation, synchronisation errors.

I. Introduction

Nano-machines have been proposed to enable future medical and biological applications such as precision drug delivery and immune system support [1]. To facilitate the operation of such systems, point-to-point molecular communication is necessary. Due to the size of the nano-machines and in vivo applications, communication via electromagnetic wave is infeasible, thus molecular diffusion is considered. In such schemes, a nano-machine transmitter is assumed to contain a storage of molecules that are released into the medium. Diffusion carries the molecules across the communication channel, which are then detected by the receiver nanomachine. Different modulation schemes have been proposed for diffusive molecular communication [2], [3]. However, extensive inter-symbol interference (ISI) due to the nature of diffusion is a major bottleneck. The effect of ISI on molecular communication is discussed in [4], [5].

Prior molecular communication works have presumed perfect time synchronisation between the transmitter and receiver [6]–[8]. To achieve synchronicity, a variety of synchronisation schemes have been proposed [9]–[13]. However, the absolute performances of these methods are limited in diffusive channels and are often high in complexity, making them

This research was funded in part by NSF grants CCF-1718560 and CCF-1817200.

prohibitive for nano-machines. To remedy this issue, a simple asynchronous detection scheme is introduced in [14] that does not require perfect synchronisation. However, as will be shown, the performance is not strong due to its simplistic approach. We will show that with a moderate increase in complexity, performance can be improved dramatically.

Herein, we presume the linear time-invariant (LTI) Poisson channel of [3], based on the additive inverse Gaussian channel model of [15], to develop the Synchronised Memory Aided Sequential Probability Ratio Test (SMASPRT). SMASPRT is an augmented version of the sequential probability ratio test (SPRT) [16]. In [17], a SPRT based transceiver, called Memory Aided Sequential Probability Ratio Test (MASPRT), where ISI is mitigated with decision feedback, was proposed and shown to offer strong improvement of asynchronous detection performance over [6] and [14]. Here, we adopt the design and analyses in [17] and offer an approximate maximum loglikelihood estimator for the synchronisation error to further improve the detection performance, hence the SMASPRT. The estimator allows SMASPRT to offer further resilience to synchronisation errors by limiting the effect of likelihood function mismatch. Additionally, we further optimise the modulating sequence to minimise the error probability. The proposed scheme is compared to that in [6] and [14]. In [6], it was shown that their approach was near-optimal for the LTI Poisson channel under the assumption of perfect synchronisation. In our testing, SMASPRT offers superior performance to both schemes in the presence of mis-synchronisation.

The main contributions of this paper are as follows; (i) we improve upon the MASPRT scheme in [17] by proposing an approximate maximum log-likelihood estimator for the synchronisation error to further improve detection performance; (ii) the Cramér-Rao bound (CRB) of the estimator is calculated and the estimator is shown to be nearly optimal for low transmission rates; (iii) our results show that SMASPRT improves asynchronous detection performance under the same data rate as the schemes proposed in [6] and [14] with a reduction in bit error ratio (BER) by a factor of 3 and 5 on average, respectively.

This paper is organised as follows: Section II and III describe the channel and transceiver models, respectively; Section IV calculates the CRB of the proposed synchronisation error estimator; Section V proposes the optimal transceiver design and Section VI discusses the numerical results based on bounding key performance metrics in the proposed design.

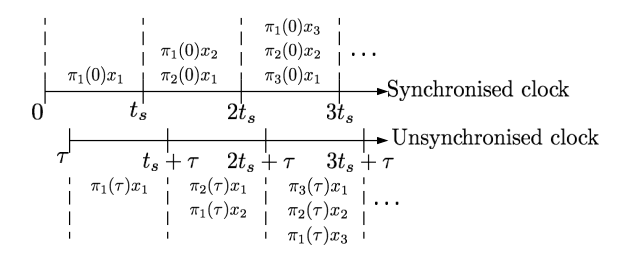


Fig. 1. Illustration of synchronisation error on sample distribution.

II. RECEIVED SIGNAL

Diffusion-based molecular communication, whereby molecules experience Brownian motion without drift, is considered and inter-molecular collisions are assumed to have negligible effects on the diffusion of molecules. Without loss of generality, we consider only one-dimensional motion. A storage device releases molecules into the channel and the number of released molecules is described by a Poisson random variable with rate x. This distribution is indicated by Poi(x). To convey a message, the transmitter releases a predefined sequence of rates. Without loss of generality, the received signal is described by the one-dimensional linear-time invariant Poisson model proposed in [3]. We assume a constant release and sampling duration denoted by t_s and the rate x_t denotes the rate associated with time slot t. Assuming that the molecules are released at the beginning of each time slot, the probability that a molecule is detected by the receiver at the tth time slot is denoted by $\pi_t(\tau)$, where τ denotes the synchronisation error between the transmitter and receiver clocks as illustrated in Figure 1. $\pi_t(\tau)$ is defined as

$$\pi_t(\tau) = 2Q\left(\frac{\rho}{\sqrt{t \cdot t_s + \tau}}\right) - 2Q\left(\frac{\rho}{\sqrt{(t-1)t_s + \tau}}\right), \quad (1)$$

where the constant $\rho \triangleq \frac{d}{\sqrt{2D}}$ summarises the relationship between the diffusion constant (D) and the distance between the transmitter and receiver (d). The standard Q function is given by $Q(a) = \int_a^\infty \frac{1}{\sqrt{2\pi}} e^{\frac{-x^2}{2}} dx$. The noise within the system is described by a homogeneous Poisson process, with rate function $\lambda(u) = \lambda_0 u$. As such, the number of molecules detected within the tth time slot is a Poisson random variable with the following distribution

$$Y_t \sim \text{Poi}(\boldsymbol{\pi}_t(\tau) \otimes \boldsymbol{x}_t + \lambda_0 t_s), \quad \forall t > 1,$$
 (2)

where $\pi_t(\tau) = [\pi_1(\tau), \pi_2(\tau), \dots, \pi_t(\tau)]$, $\mathbf{x}_t = [x_1, x_2, \dots, x_t]$ and \otimes denotes the convolution operation. The samples are independent and it is assumed that the synchronisation error $\tau \geq 0$ for simplicity.

For simplicity, we consider binary signalling where a source symbol, s_j , maps to a modulation signal denoted by $\mathbf{x}_j = [x_{1|j}, x_{2|j}, \dots, x_{N|j}] \in \mathbb{R}^N$, $j = \{0,1\}$, where N is the modulation signal length. The transmission rate is defined as $R = \frac{1}{t_s \cdot N}$. It is assumed that $||\mathbf{x}_j||_2 \leq P$, where P is the power constraint, and that the receiver is unaware of the true value of τ , leading to likelihood mismatch. Due to the

the complexity of the channel model with respect to τ , joint optimisation of the detection performance and estimator is intractable. Therefore, in the sequel, we shall focus on the optimisation of \mathbf{x}_j for detection performance and data rate assuming $\tau=0$ and provide an approximate maximum log-likelihood estimator for τ .

III. SYNCHRONISED MEMORY AIDED SPRT

We consider the sequential probability ratio test (SPRT) [16] as the basis for our detection strategy. SPRT samples the signal and calculates the likelihood ratio. When confident, it terminates with a decision, otherwise another sample is taken. We provide three key modifications to the original SPRT formulation for our context: (i) a memory of B bits is used to compensate for ISI; (ii) an approximate maximum log-likelihood estimator for the synchronisation error τ is proposed to obtain a more accurate estimate of the likelihood ratio; (iii) a trunction rule is introduced to avoid sampling into subsequent channel symbols; hence the SMASPRT.

Let $s^n \in \{s_0, s_1\}$ be the *n*th source symbol being conveyed and $\mathbf{y}_m^n = [y_1^n, y_2^n, \dots, y_m^n]$ be the vector of samples observed for that symbol, the likelihood ratio function is given by

$$L_m(\mathbf{y}_m^n, \bar{\tau}_{n-1}) = \frac{p_{\mathbf{y}_m^n|s_1}(\bar{\tau}_{n-1})}{p_{\mathbf{y}_m^n|s_0}(\bar{\tau}_{n-1})},$$

where $p_{\mathbf{y}_m^n|s_j}(\bar{\tau}_{n-1})$ is the joint Poisson probability mass function for symbol s_j as implied by Equation (2) and $\bar{\tau}_{n-1}$ is the synchronisation error estimate obtained from the previous symbol s^{n-1} .

Let $E[Y_m^n|s_j] = \bar{\lambda}_{m|j}^n(\mathbf{x}_j,\tau)$, for each sample y_m^n . If $L_m(\mathbf{y}_m^n) \geq 1$, then an estimate of the synchronisation error $\hat{\tau}_m^n$ is calculated using $\bar{\lambda}_{m|1}^n(\mathbf{x}_1,\tau)$ and stored; otherwise, $\bar{\lambda}_{m|0}^n(\mathbf{x}_0,\tau)$ is used. Consider the maximum log-likelihood estimator

$$\begin{split} &\tilde{\tau}_m^n(y_m^n) \\ &= \operatorname*{arg\,max}_{\tau} \log p_{Y_m^n|s_j}(y_m^n; \mathbf{x}_j, \tau) \\ &= \operatorname*{arg\,max}_{\tau} y_m^n \log(\bar{\lambda}_{m|j}^n(\mathbf{x}_j, \tau)) - \bar{\lambda}_{m|j}^n(\mathbf{x}_j, \tau) - \log(y_m^n!). \end{split}$$

The solution to $\tilde{\tau}_m^n(y_m^n)$ is derived by

$$\begin{split} &\frac{\partial}{\partial \tau} \left[y_m^n \log(\bar{\lambda}_{m|j}^n(\mathbf{x}_j, \tau)) - \bar{\lambda}_{m|j}^n(\mathbf{x}_j, \tau) - \log(y_m^n!) \right] \\ &= y_m^n \frac{\partial}{\partial \tau} \bar{\lambda}_{m|j}^n(\mathbf{x}_j, \tau) - \frac{\partial}{\partial \tau} \bar{\lambda}_{m|j}^n(\mathbf{x}_j, \tau) = 0 \\ &\Rightarrow \bar{\lambda}_{m|j}^n(\mathbf{x}_j, \tau) - y_m^n = 0. \end{split}$$

Hence, the estimate is such that $\bar{\lambda}^n_{m|j}(\mathbf{x}_j,\tilde{\tau}^n_m(y^n_m))-y^n_m=0$. To reduce the complexity of solving this equation, we fit the function $\bar{\lambda}^n_{m|j}(\mathbf{x}_j,\tau)$ to an exponential function due to the convex non-increasing nature of $\bar{\lambda}^n_{m|j}(\mathbf{x}_j,\tau)$ with respect to $\tau\geq 0$. Let $\bar{\lambda}^n_{m|j}(\mathbf{x}_j,\tau)\approx a^n_m e^{\tau^n_m \tau}$, we minimise the least-squares objective function of the log-likelihood function

$$\underset{\log a_m^n, r_m^n}{\arg \min} \sum_{k=1}^{i} [\log \bar{\lambda}_{m|j}^n(\mathbf{x}_j, \tau_k) - \log a_m^n - r_m^n \tau_k]^2,$$

where $\tau_k, k=1,2,\ldots,l$ are sampling points on the function $\bar{\lambda}^n_{m|j}(\mathbf{x}_j,\tau)$. The solutions to the coefficients $[\log a^n_m, r^n_m]$ are

$$r_{m}^{n} = \frac{\sum_{k=1}^{l} \tau_{k} \log \bar{\lambda}_{m|j}^{n}(\mathbf{x}_{j}, \tau_{k})}{\sum_{k=1}^{l} \tau_{k}^{2} - \frac{1}{l} (\sum_{k=1}^{l} \tau_{k})^{2}} - \frac{\frac{1}{l} (\sum_{k=1}^{l} \tau_{k}) (\sum_{k=1}^{l} \log \bar{\lambda}_{m|j}^{n}(\mathbf{x}_{j}, \tau_{k}))}{\sum_{k=1}^{l} \tau_{k}^{2} - \frac{1}{l} (\sum_{k=1}^{l} \tau_{k})^{2}}$$

$$\log a_{m}^{n} = \frac{1}{l} \sum_{k=1}^{l} \log \bar{\lambda}_{m|j}^{n}(\mathbf{x}_{j}, \tau_{k}) - \frac{r_{m}^{n}}{l} \sum_{k=1}^{l} \tau_{k}.$$

Hence, the approximate maximum log-likelihood estimator is

$$\hat{\tau}_m^n(y_m^n) = \frac{\log y_m^n - \log a_m^n}{r_m^n}.$$
 (3)

We observe that the function $\bar{\lambda}^n_{m|j}(\mathbf{x}_j,\tau)$ is different for each sample y^n_m , due to r^n_m and a^n_m being dependent on n and m. Therefore, we average over all past estimates to obtain $\bar{\tau}_n = \frac{1}{i}((i-m)\bar{\tau}_{n-1} + \sum_{k=1}^m \hat{\tau}^n_k(y^n_k))$ if the algorithm terminates at the ith global sample (i.e. the ith sample it takes since the beginning of time) and use this in the next symbol detection to calculate its likelihood ratio more accurately.

When confident, if m < N, where N is the modulation signal length, the decision rule is given by

$$\delta(L_m(\mathbf{y}_m^n, \bar{\tau}_{n-1})) = \begin{cases} s_0, & L_m(\mathbf{y}_m^n, \bar{\tau}_{n-1}) \le A \\ s_1, & L_m(\mathbf{y}_m^n, \bar{\tau}_{n-1}) \ge B \end{cases} \quad (4)$$
sample, else.

The constants A and B are given by $A = \frac{\beta}{1-\alpha}$, $B = \frac{1-\beta}{\alpha}$ (as in [16]), where α is the false alarm rate and β is the miss probability. If the SMASPRT does not terminate by m = N, a truncation rule based on the minimum distance rule is applied to prevent sampling into the subsequent channel symbol:

$$\begin{split} & \delta(L_N(\mathbf{y}_N^n, \bar{\tau}_{n-1})) \\ & = \begin{cases} s_0, & |L_N(\mathbf{y}_N^n, \bar{\tau}_{n-1}) - A| < |L_N(\mathbf{y}_N^n, \bar{\tau}_{n-1}) - B| \\ s_1, & |L_N(\mathbf{y}_N^n, \bar{\tau}_{n-1}) - A| \ge |L_N(\mathbf{y}_N^n, \bar{\tau}_{n-1}) - B|. \end{cases} \end{split}$$

The exact likelihood ratio $L_m(\mathbf{y}_m^n, \tau)$ and $\bar{\lambda}_{m|j}^n(\mathbf{x}_j, \tau)$ requires the knowledge of the joint likelihood function of the samples $p_{\mathbf{y}_{m}^{n}|s_{j}}(\tau)$ for $j \in \{0,1\}$. However, since the channel exhibits memory of all past transmissions, knowledge of all past diffusion rates would be needed to calculate the exact likelihood function, which is infeasible. To remedy this issue, a memory of B bits is embedded in the receiver, such that the receiver can store B past decoded source symbols at the *n*th symbol, denoted by $M_n = \{\hat{s}_{n-1}, \hat{s}_{n-2}, \dots, \hat{s}_{n-B}\}.$ The receiver is then able to estimate the likelihood function, denoted by $\hat{p}_{\mathbf{y}_{m}^{n}|s_{i}}(\bar{\tau}_{n-1})$, up to $B \cdot N + m$ time slots in the past by appropriately using the mapping $s_i \to \mathbf{x}_i$. Assuming the source symbols in the memory were decoded correctly, the more memory the receiver possesses, the more accurate the likelihood ratio and the lower the error probability for SMASPRT. It should be noted here that the desired α and β can only be achieved if the likelihood ratio is calculated exactly. Since an estimate is used here, the probability of error will be greater than those set by α and β , depending on how much memory is used and the synchronisation error.

IV. CRAMÉR-RAO BOUND (CRB)

We consider the maximum log-likelihood estimator $\tilde{\tau}_m^n(y_m^n)$ for the purpose of calculating the Cramér-Rao bound (CRB). To verify that the CRB exists, we first check the regularity condition. That is

$$E\left[\frac{\partial}{\partial \tau} \log p_{Y_m^n|s_j}(y_m^n; \mathbf{x}_j, \tau)\right]$$

$$=E\left[\frac{\partial}{\partial \tau} y_m^n \log(\bar{\lambda}_{m|j}^n(\mathbf{x}_j, \tau)) - \bar{\lambda}_{m|j}^n(\mathbf{x}_j, \tau) - \log(y_m^n!)\right]$$

$$=E\left[y_m^n \frac{\partial}{\partial \tau} \bar{\lambda}_{m|j}^n(\mathbf{x}_j, \tau) - \frac{\partial}{\partial \tau} \bar{\lambda}_{m|j}^n(\mathbf{x}_j, \tau)\right]$$

$$=\bar{\lambda}_{m|j}^n(\mathbf{x}_j, \tau) \frac{\partial}{\partial \tau} \bar{\lambda}_{m|j}^n(\mathbf{x}_j, \tau) - \frac{\partial}{\partial \tau} \bar{\lambda}_{m|j}^n(\mathbf{x}_j, \tau) = 0.$$

Next, let $J_{y_m^n}(\tau)$ be the Fisher information in y_m^n about τ , then the CRB of the estimate $\tilde{\tau}_m^n(y_m^n)$ is computed as follows

$$\frac{\partial^{2}}{\partial \tau^{2}} \log p_{Y_{m}^{n}|s_{j}}(y_{m}^{n}; \mathbf{x}_{j}, \tau)
= \frac{\partial^{2}}{\partial \tau^{2}} \left[y_{m}^{n} \log(\bar{\lambda}_{m|j}^{n}(\mathbf{x}_{j}, \tau)) - \bar{\lambda}_{m|j}^{n}(\mathbf{x}_{j}, \tau) - \log(y_{m}^{n}!) \right]
= \frac{\partial}{\partial \tau} \left[y_{m}^{n} \frac{\frac{\partial}{\partial \tau} \bar{\lambda}_{m|j}^{n}(\mathbf{x}_{j}, \tau)}{\bar{\lambda}_{m|j}^{n}(\mathbf{x}_{j}, \tau)} - \frac{\partial}{\partial \tau} \bar{\lambda}_{m|j}^{n}(\mathbf{x}_{j}, \tau) \right]
= y_{m}^{n} \frac{\bar{\lambda}_{m|j}^{n}(\mathbf{x}_{j}, \tau) \frac{\partial^{2}}{\partial \tau^{2}} \bar{\lambda}_{m|j}^{n}(\mathbf{x}_{j}, \tau) - (\frac{\partial}{\partial \tau} \bar{\lambda}_{m|j}^{n}(\mathbf{x}_{j}, \tau))^{2}}{(\bar{\lambda}_{m|j}^{n}(\mathbf{x}_{j}, \tau))^{2}}
- \frac{\partial^{2}}{\partial \tau^{2}} \bar{\lambda}_{m|j}^{n}(\mathbf{x}_{j}, \tau)
\Rightarrow J_{y_{m}^{n}}(\tau) = -E \left[\frac{\partial^{2}}{\partial \tau^{2}} \log p_{Y_{m}^{n}|s_{j}}(y_{m}^{n}; \mathbf{x}_{j}, \tau) \right]
= \frac{(\frac{\partial}{\partial \tau} \bar{\lambda}_{m|j}^{n}(\mathbf{x}_{j}, \tau))^{2}}{\bar{\lambda}_{m|i}^{n}(\mathbf{x}_{j}, \tau)}.$$

Therefore, the CRB of the estimate $\tilde{\tau}_m^n(y_m^n)$ is

$$E[(\tilde{\tau}_m^n(y_m^n) - \tau)^2] \ge \frac{1}{J_{y_m^n}(\tau)} = \frac{\bar{\lambda}_{m|j}^n(\mathbf{x}_j, \tau)}{(\frac{\partial}{\partial \tau} \bar{\lambda}_{m|j}^n(\mathbf{x}_j, \tau))^2}.$$

As the final estimate is the empirical mean of each sample estimate, we have the following modified bound

$$\frac{1}{m} \sum_{k=1}^m E[(\tilde{\tau}_k^n(y_k^n) - \tau)^2] \ge \frac{1}{m} \sum_{k=1}^m \frac{\lambda_{k|j}^n(\mathbf{x}_j, \tau)}{(\frac{\partial}{\partial \tau} \bar{\lambda}_{k|j}^n(\mathbf{x}_j, \tau))^2}.$$

It should be noted here that this result only holds if the estimator is unbiased, which the maximum log-likelihood estimator $\tilde{\tau}_m^n(y_m^n)$ satisfies. However, since we are using the approximate maximum log-likelihood estimator $\hat{\tau}_m^n(y_m^n)$, which is a worse estimator compared to $\tilde{\tau}_m^n(y_m^n)$, the mean squared error (MSE) $E[(\hat{\tau}_m^n(y_m^n)-\tau)^2]\geq E[(\tilde{\tau}_m^n(y_m^n)-\tau)^2]$, resulting in a looser bound.

V. TRANSCEIVER OPTIMISATION

In [17], the error probability $P_e = P[s_0]P[s_1|s_0] +$ $P[s_1]P[s_0|s_1]$ and the expected stopping time of SMASPRT were bounded to provide the framework for transceiver optimisation. In particular, the result that the optimal value for \mathbf{x}_0 is $\mathbf{x}_0 = \mathbf{0}$ (vector of zeros) was adopted from [6] and it was assumed that $P[s_1|s_0] >> P[s_0|s_1]$ due to the ISI of past s_1 transmissions. Therefore, only \mathbf{x}_1 has to be optimised. We provide Proposition 1 and 2 from [17] to formulate our optimisation problem:

Proposition 1: Assuming an LTI Poisson channel as described in Equation (2) and that $\mathbf{x}_0 = \mathbf{0}$. Let $E[Y_k^n|s_j] = \bar{\lambda}_{k|j}^n(\mathbf{x}_1,\tau) = \bar{\lambda}_{k|j}^C + \bar{\lambda}_k^{ISI} + n_0$, where $\bar{\lambda}_{k|j}^C$ denotes the diffusion rates transmitted for the current source symbol, $\bar{\lambda}_k^{ISI}$ denotes the ISI terms, and $n_0 = \lambda_0 t_s$. Then $P[s_1|s_0]$ can be bounded as follows:

$$P[s_1|s_0] \leq \bar{\lambda}_{1|1}^C + \mu \sum_{k=2}^N \bar{\lambda}_{k|1}^C$$

$$= \left(\pi_1(\tau) + \mu \sum_{i=2}^N \pi_i(\tau)\right) x_{1|1} + \mu \sum_{k=1}^{N-1} x_{k+1|1} \sum_{i=1}^{N-k} \pi_i(\tau),$$

where
$$\mu = P \left[\frac{\log(A) + 2\pi_1(\tau)x_{1|1}}{\log\left(\frac{x_{1|1} + \lambda_1^{TSI} + n_0}{n_0 + \lambda_1^{TSI}}\right)} < y_1 < \frac{\log(B) + 2\pi_1(\tau)x_{1|1}}{\log\left(\frac{x_{1|1} + \lambda_1^{TSI} + n_0}{n_0 + \lambda_1^{TSI}}\right)} \right]$$

and $\left[A,B\right]$ are thresholds described in Equation

Proposition 2: Let $E[Y_k^n|s_j] = \bar{\lambda}_{k|j}^n(\mathbf{x}_j, \tau)$. There exists $\epsilon > 0$ and $T_j(\epsilon)$ for $j \in \{0, 1\}$, such that:

$$\sum_{k=T_{1}(\epsilon)+1}^{\infty} \frac{1}{k} \left\{ \bar{\lambda}_{k|1}^{n}(\mathbf{x}_{1}, \tau) \left[\log \left(\frac{\lambda_{k|1}^{n}(\mathbf{x}_{1}, \tau)}{\bar{\lambda}_{k|0}^{n}(\mathbf{x}_{1}, \tau)} \right) - 1 \right] + \bar{\lambda}_{k|0}^{n}(\mathbf{x}_{1}, \tau) \right\} \leq \epsilon$$

$$\sum_{k=T_{1}(\epsilon)+1}^{\infty} \frac{1}{k} \left\{ \bar{\lambda}_{1|0}^{n}(\mathbf{x}_{1}, \tau) \left[\log \left(\frac{\bar{\lambda}_{k|0}^{n}(\mathbf{x}_{1}, \tau)}{\bar{\lambda}_{k|0}^{n}(\mathbf{x}_{1}, \tau)} \right) - 1 \right] + \bar{\lambda}_{1|1}^{n}(\mathbf{x}_{1}, \tau) \right\} \leq \epsilon$$

$$\sum_{k=T_0(\epsilon)+1}^{\infty} \frac{1}{k} \left\{ \bar{\lambda}_{k|0}^n(\mathbf{x}_1, \tau) \left[\log \left(\frac{\bar{\lambda}_{k|0}^n(\mathbf{x}_1, \tau)}{\bar{\lambda}_{k|1}^n(\mathbf{x}_1, \tau)} \right) - 1 \right] + \bar{\lambda}_{k|1}^n(\mathbf{x}_1, \tau) \right\} \leq \epsilon,$$

$$\frac{\log B}{T_1(\epsilon)} \leq \sum_{k=1}^{T_1(\epsilon)} \frac{1}{k} \left\{ \bar{\lambda}_{k|1}^n(\mathbf{x}_1, \tau) \left[\log \left(\frac{\bar{\lambda}_{k|1}^n(\mathbf{x}_1, \tau)}{\bar{\lambda}_{k|0}^n(\mathbf{x}_1, \tau)} \right) - 1 \right] + \bar{\lambda}_{k|0}^n(\mathbf{x}_1, \tau) \right\}$$

$$\frac{\log A^{-1}}{T_0(\epsilon)} \leq \sum_{k=1}^{T_0(\epsilon)} \frac{1}{k} \left\{ \bar{\lambda}_{k|0}^n(\mathbf{x}_1,\tau) \left[\log \left(\frac{\bar{\lambda}_{k|0}^n(\mathbf{x}_1,\tau)}{\bar{\lambda}_{k|1}^n(\mathbf{x}_1,\tau)} \right) - 1 \right] + \bar{\lambda}_{k|1}^n(\mathbf{x}_1,\tau) \right\}.$$

Combining Propositions 1 and 2, we assume that all past transmitted source symbols are s_1 leading to maximal ISI. The optimisation problem is formulated by P1:

$$\hat{\mathbf{x}}_1 = \arg\min_{\mathbf{x}_1} \left(\pi_1(\tau) + \mu \sum_{i=2}^{N} \pi_i(\tau) \right) x_{1|1} + \mu \sum_{k=1}^{N-1} x_{k+1|1} \sum_{i=1}^{N-k} \pi_i(\tau)$$

$$\text{s.t.} \sum_{k=1}^{T_1(\epsilon)} \frac{1}{k} \bigg\{ \bar{\lambda}_{k|1}^n(\mathbf{x}_1, \tau) \bigg[\log \bigg(\frac{\bar{\lambda}_{k|1}^n(\mathbf{x}_1, \tau)}{\bar{\lambda}_{k|0}^n(\mathbf{x}_1, \tau)} \bigg) - 1 \bigg] + \bar{\lambda}_{k|0}^n(\mathbf{x}_1, \tau) \bigg\} \geq \frac{\log B}{T_1(\epsilon)}$$

$$\sum_{k=1}^{T_0(\epsilon)} \frac{1}{k} \left\{ \bar{\lambda}_{k|0}^n(\mathbf{x}_1, \tau) \left[\log \left(\frac{\bar{\lambda}_{k|0}^n(\mathbf{x}_1, \tau)}{\bar{\lambda}_{k|1}^n(\mathbf{x}_1, \tau)} \right) - 1 \right] + \bar{\lambda}_{k|1}^n(\mathbf{x}_1, \tau) \right\} \ge \frac{-\log A}{T_0(\epsilon)}$$

$$||\mathbf{x}_1||_2 \le P,$$

where $\bar{\lambda}_{k|1}^n(\mathbf{x}_1,\tau) = \boldsymbol{\pi}_{k+N\cdot B}(\tau) \otimes [\mathbf{x}_1;\ldots;\mathbf{x}_1;\mathbf{x}_1(1:k)] +$ $\lambda_0 t_s$ and $\bar{\lambda}_{k|0}^n(\mathbf{x}_1, \tau) = \boldsymbol{\pi}_{k+N \cdot B}(\tau) \otimes [\mathbf{x}_1; \dots; \mathbf{x}_1; \mathbf{0}(1:k)] + \lambda_0 t_s$. Here, $[\mathbf{x}_1; \dots; \mathbf{x}_1] \in \mathbb{R}^{N \cdot B}$ is the concatenated vector of $B \mathbf{x}_1$'s, and the notation (1:k) denotes taking the first k elements of a vector. This can be solved using traditional optimisation algorithms such as the interior-point method. We emphasise that this optimisation process only needs to be done once offline; it does not contribute to transmitter complexity.

VI. NUMERICAL RESULTS TABLE I EXAMPLE NUMERICAL RESULTS.

	t_s (s)	τ (s)	\bar{T}_0	\bar{T}_1	$T_0(\epsilon)$	$T_1(\epsilon)$	$ \hat{\mathbf{x}}_{1} _{2}$
ĺ	0.1	0	4.5	3.2	5	5	56.1
ĺ	0.1	0.5	5.0	10.3	5	5	56.1
	0.025	0	4.5	7.2	5	5	99.6

The following parameters are used for simulation: $\alpha =$ $\beta = 10^{-3}, \ \rho = \sqrt{0.3}, \ N = 20, \ \lambda_0 = 4 \text{ molecules/s},$ $T_0(\epsilon) = T_1(\epsilon) = 5$ and P = 100. The transmission rate is controlled by changing the sampling rate t_s . 100 packets of length 100 bits are considered to obtain an average BER. We solve the optimisation problem presented in Section V, assuming $\tau = 0$, using the interior-point method in MATLAB. It is found that as the sampling rate increases, the magnitude of the vector $\hat{\mathbf{x}}_1$ increases. In the presence of synchronisation error, let T_0 and T_1 denote the empirical mean of the stopping times under s_0 and s_1 , respectively, it is found that T_0 stays roughly the same while \bar{T}_1 increases. Examples of simulation results are shown in Table I. This follows from the decay of the hitting probabilities; as t_s decreases or as τ increases, the hitting probabilities decrease. Therefore, either the transmitter compensates by increasing the number of molecules transmitted in the case of increasing transmission rate, or the receiver requires more samples to converge in the case of increasing synchronisation error. Since $x_0 = 0$, synchronisation errors affect the expected stopping time of the algorithm under s_0 only slightly.

The memory-limited decision aided (MLDA) decoder and the asynchronous detector with decision feedback (ADDF), proposed in [6] and [14], respectively, are used as competing schemes to show that SMASPRT can perform similarly to MLDA under synchronous scenarios and improve asynchronous detection performance over both schemes. As neither MLDA nor ADDF attempt to estimate the synchronisation error τ , the approximate maximum log-likelihood estimator for τ is incorporated into MLDA and ADDF for a fair comparison. MASPRT is also compared with SMASPRT to show the improvement in asynchronous detection performance using the approximate maximum log-likelihood estimator.

The MLDA transmitter modulates the signal by mapping $s_i \in \mathbb{R} \to x_i \in \mathbb{R}$, for $j \in \{0,1\}$. For each sample y_i , MLDA makes a decision using an estimate of the ISI $(\hat{\lambda}_i^{ISI})$ from its memory and the maximum log-likelihood estimator $\hat{x}(y_i) = \max P[y_i|x_j, \hat{\lambda}_i^{ISI}]$. A threshold can be derived by equating $P[y_i|x_1,\hat{\lambda}_i^{ISI}] = P[y_i|x_0,\hat{\lambda}_i^{ISI}]$, such that

$$\gamma = \frac{\pi_1(\tau)(x_1 - x_0)}{\log\left(\frac{\pi_1(\tau)x_1 + \hat{\lambda}_i^{ISI} + n_0}{\pi_1(\tau)x_0 + \hat{\lambda}_i^{ISI} + n_0}\right)}.$$

The detection rule is then formulated as:

$$\delta(y_i) = \begin{cases} s_0, & y_i < \gamma \\ s_1, & y_i \ge \gamma. \end{cases}$$

In the paper, it is shown that this scheme is near optimal under synchronous transceivers. This is found to be true as our simulations showed MLDA to be best in terms of BER among the schemes considered here over a range of transmission rates for $\tau=0$ s.

ADDF oversamples each source symbol and thresholds the maximum sample within the window of observation to determine if the transmitted source symbol is s_0 or s_1 . The transmitter modulation mapping is the same as MLDA. Consider N samples within a particular source symbol duration, $[y_1, y_2, \ldots, y_N]$, the receiver subtracts the estimated expected ISI $(\hat{\lambda}_i^{ISI})$ using its memory, and finds the maximum sample within the window of observation:

$$y_{max} = \max_{i \in \{1, \dots, N\}} y_i - \hat{\lambda}_i^{ISI}.$$

 y_{max} is then thresholded to decide between s_0 and s_1

$$\delta(y_{max}) = \begin{cases} s_0, & y_{max} < \eta \\ s_1, & y_{max} \ge \eta. \end{cases}$$

If the synchronisation error is small, the maximum will exist within the window of observation. The decision threshold η is optimised by calculating the probability of error for a range of η 's and choosing the value that gives the lowest error probability.

Figure 2 shows the CRB and the MSE of the mean estimator $\bar{\tau}_n$ (as described in Section IV) for different transmission rates. 5 evenly spaced sampling points between [0,2]s on the function $\bar{\lambda}_{m|j}^{n}(\mathbf{x}_{j},\tau)$ is considered, (i.e. l=5). As we observe that in Proposition 1, the upper bound for the error probability $P[s_1|s_0]$ is essentially a linear combination of the diffusion rates x_1 for a given transmission rate R. Therefore, comparing the CRB and MSE for different transmission rates offers an insight to the performance of the estimator. It can be observed from Figure 2 that as the transmission rate increases, the CRB increases slightly but the MSE increases much more significantly, resulting in a looser bound at high transmission rates. This is reflected in Figure 4, as the BER increases with transmission rate, indicating that the synchronisation estimates are worse in this regime. The increase in MSE is due to both the increase in ISI as a function of rate and the approximate nature of the estimator which results in larger bias for larger rate. As a result, the estimates $\hat{\tau}_m^n(y_m^n)$ are worse at high transmission rates. However, as Figure 4 shows, despite the large MSE, SMASPRT yields superior performance results at high transmission rates, compared to MLDA and ADDF using the same estimator.

Figure 3 shows the improvement of MLDA and MASPRT when incoporated with the estimator $\hat{\tau}_m^n(y_m^n)$. Here, "MLDA

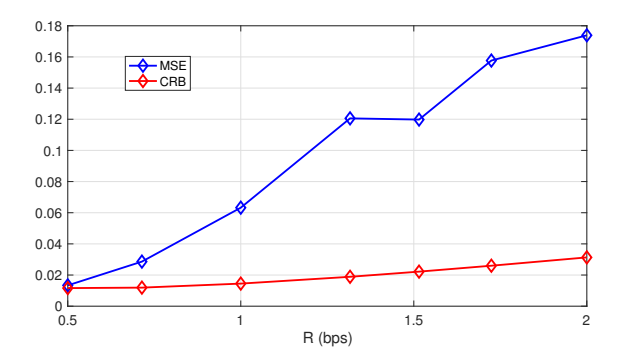


Fig. 2. Plot of transmission rate (R) against CRB and MSE of the estimator $\bar{\tau}_n$ for $\tau = 0.1$ s. Each transmission rate is simulated with the optimal $\hat{\mathbf{x}}_1$.

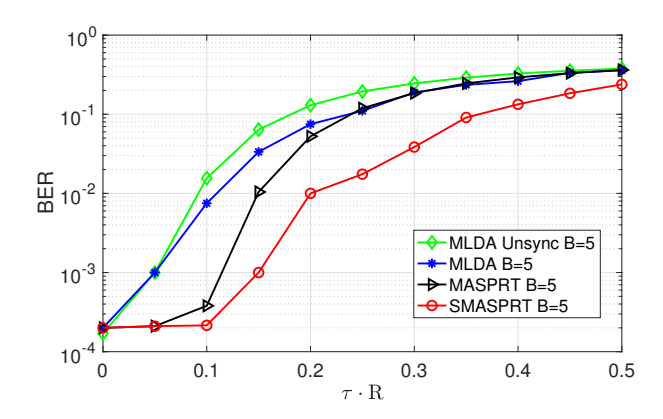


Fig. 3. Numerical results of plotting normalised synchronisation error $(\tau \cdot R)$ against BER for synchronised and unsynchronised schemes. Here, "MLDA Unsync" refers to MLDA without estimating the synchronisation error τ . Transmission rate is set at 0.5 bps. All schemes here are simulated with the optimised $\hat{\mathbf{x}}_1$ sequence for R=0.5 bps.

Unsync" refers to MLDA without estimating the synchronisation error τ . As can be seen by the results, the use of the estimator improves the ISI mitigation capabilities of both algorithms. SMASPRT performs noticeably better than MASPRT as the likelihood ratio is calculated more accurately. MLDA can also be seen to improve, but less so than SMASPRT.

Figure 4 shows the BER at different transmission rates. The diffusion rate sequence \mathbf{x}_1 is optimised for each transmission rate. The synchronisation error is set at $\tau=0.1$ s. In all scenarios, SMASPRT performs better than MLDA and ADDF in the presence of synchronisation error. On average, SMASPRT reduces the BER by a factor of 3 and 14 compared to MLDA and ADDF, respectively, in this test. SMASPRT also improves significantly with increasing memory, whereas MLDA and ADDF improve only marginally. The ADDF scheme performs significantly worse than both MLDA and SMASPRT due to the fact that it only considers the first moment of the ISI distribution.

Figure 5 shows the resilience of each scheme to synchronisation error τ . Here, R=0.5 bps and \mathbf{x}_1 is optimised for this transmission rate. The results show that SMASPRT is able to maintain a roughly constant BER up to approximately $\tau=0.2$ s, whereas the MLDA scheme does not have this resilience. On average, SMASPRT reduces the BER by a factor

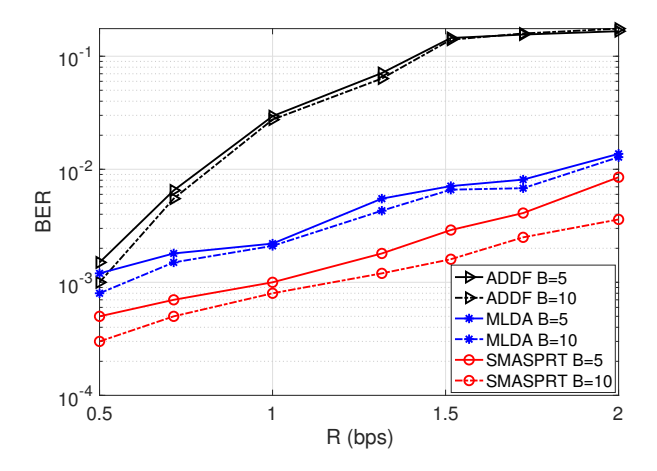


Fig. 4. Plotting transmission rate (R) against BER for $\tau=0.1s$. All schemes here are simulated with the optimised $\hat{\mathbf{x}}_1$ sequences for each transmission rate assuming $\tau=0$ and with the estimator $\hat{\tau}_n^n(y_n^n)$ incorporated.

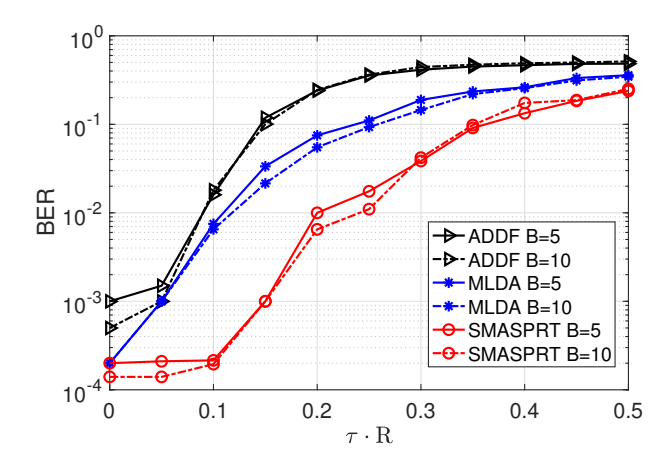


Fig. 5. Numerical results of plotting normalised synchronisation error (τ ·R) against BER. Transmission rate is set at 0.5 bps. All schemes here are simulated with the optimised $\hat{\mathbf{x}}_1$ sequence for R=0.5 bps and with the estimator $\hat{\tau}_m^n(y_m^n)$ incorporated.

of 3 and 5 compared to MLDA and ADDF, respectively, in this test. The performance improvement comes from the fact that SMASPRT is designed to stop before the sampling limit. Thus, when a synchronisation error is present, the accumulation of errors in the calculation of LLR is lower compared to MLDA, resulting in a lower error probability. ADDF can also be seen to tolerate some synchronisation errors, but it's overall higher BER means it cannot perform as well as MLDA or SMASPRT.

VII. CONCLUSIONS

A transceiver design for molecular communication, called *Synchronised Memory Aided Sequential Probability Ratio Test* (SMASPRT), based on SPRT has been proposed in this paper. Bounds on the error probability and expected stopping times were adopted from prior work and used to optimise the modulation signal design. A synchronisation scheme based on an approximate maximum log-likelihood estimator was proposed. The mean squared error of the estimator was compared with the Cramér-Rao bound for different transmission

rates and the estimator was shown to be nearly optimal for low transmission rates. SMASPRT improves asynchronous detection performance under the same data rate as MLDA and ADDF with a reduction in BER by a factor of 3 and 5 on average, respectively.

REFERENCES

- T. Nakano, M. J. Moore, F. Wei, A. V. Vasilakos, and J. Shuai, "Molecular Communication and Networking: Opportunities and Challenges," *IEEE Transactions on NanoBioscience*, vol. 11, no. 2, pp. 135–148, Jun 2012.
- [2] M. S. Kuran, H. B. Yilmaz, T. Tugcu, and I. F. Akyildiz, "Modulation Techniques for Communication via Diffusion in Nanonetworks," in 2011 IEEE International Conference on Communications (ICC), Jun. 2011, pp. 1–5.
- [3] H. Arjmandi, A. Gohari, M. N. Kenari, and F. Bateni, "Diffusion-Based Nanonetworking: A New Modulation Technique and Performance Analysis," *IEEE Communications Letters*, vol. 17, no. 4, pp. 645–648, Apr. 2013.
- [4] M. J. Moore, T. Suda, and K. Oiwa, "Molecular Communication: Modeling Noise Effects on Information Rate," *IEEE Transactions on NanoBioscience*, vol. 8, no. 2, pp. 169–180, Jun. 2009.
- [5] M. . Kuran, H. B. Yilmaz, T. Tugcu, and I. F. Akyildiz, "Interference effects on modulation techniques in diffusion based nanonetworks," *Nano Communication Networks*, vol. 3, no. 1, pp. 65–73, Mar. 2012. [Online]. Available: http://www.sciencedirect.com/science/article/pii/S1878778912000063
- [6] R. Mosayebi, H. Arjmandi, A. Gohari, M. Nasiri-Kenari, and U. Mitra, "Receivers for Diffusion-Based Molecular Communication: Exploiting Memory and Sampling Rate," *IEEE Journal on Selected Areas in Communications*, vol. 32, no. 12, pp. 2368–2380, Dec. 2014.
- [7] M. Movahednasab, M. Soleimanifar, A. Gohari, M. Nasiri-Kenari, and U. Mitra, "Adaptive Transmission Rate With a Fixed Threshold Decoder for Diffusion-Based Molecular Communication," *IEEE Transactions on Communications*, vol. 64, no. 1, pp. 236–248, Jan. 2016.
- [8] A. Zare, A. Jamshidi, and A. Keshavarz-Haddad, "Receiver design for pulse position modulation technique in diffusion-based molecular communication," in 2017 IEEE 4th International Conference on Knowledge-Based Engineering and Innovation (KBEI), Dec. 2017, pp. 0729–0733.
- [9] B. K. Hsu, P. C. Chou, C. H. Lee, and P. C. Yeh, "Training-based synchronization for quantity-based modulation in inverse Gaussian channels," in 2017 IEEE International Conference on Communications (ICC), May 2017, pp. 1–6.
- [10] V. Jamali, A. Ahmadzadeh, and R. Schober, "Symbol synchronization for diffusive molecular communication systems," in 2017 IEEE International Conference on Communications (ICC), May 2017, pp. 1–7.
- [11] L. Lin, C. Yang, M. Ma, S. Ma, and H. Yan, "A Clock Synchronization Method for Molecular Nanomachines in Bionanosensor Networks," *IEEE Sensors Journal*, vol. 16, no. 19, pp. 7194–7203, Oct. 2016.
- [12] H. ShahMohammadian, G. G. Messier, and S. Magierowski, "Blind Synchronization in Diffusion-Based Molecular Communication Channels," *IEEE Communications Letters*, vol. 17, no. 11, pp. 2156–2159, Nov. 2013
- [13] J. Lee, M. Kim, and D. Cho, "Asynchronous Detection Algorithm for Diffusion-Based Molecular Communication in Timing Modulation Channel," *IEEE Communications Letters*, vol. 19, no. 12, pp. 2114– 2117, Dec. 2015.
- [14] A. Noel and A. W. Eckford, "Asynchronous peak detection for demodulation in molecular communication," in 2017 IEEE International Conference on Communications (ICC), May 2017, pp. 1–6.
- [15] K. V. Srinivas, A. W. Eckford, and R. S. Adve, "Molecular Communication in Fluid Media: The Additive Inverse Gaussian Noise Channel," *IEEE Transactions on Information Theory*, vol. 58, no. 7, pp. 4678–4692. Jul. 2012.
- [16] A. Wald, "Sequential Tests of Statistical Hypotheses," The Annals of Mathematical Statistics, vol. 16, no. 2, pp. 117–186, 1945.
- [17] T.-Y. Tung and U. Mitra, "SPRT Based Transceiver for Molecular Communications," arXiv:1810.06730 [eess.SP], Oct. 2018. [Online]. Available: https://arxiv.org/abs/1810.06730